HHS Public Access

Author manuscript

J Clin Immunol. Author manuscript; available in PMC 2017 August 15.

Published in final edited form as:

J Clin Immunol. 2016 October ; 36(7): 641–648. doi:10.1007/s10875-016-0312-3.

Severe Early-Onset Combined Immunodeficiency due to Heterozygous Gain-of-Function Mutations in *STAT1*

Safa Baris[1,*], **Fayhan Alroqi**[2,*], **Ayca Kiykim**[1], **Elif Karakoc-Aydiner**[1], **Ismail Ogulur**[1], **Ahmet Ozen**[1], **Louis-Marie Charbonnier**[2], **Mustafa Bakır**[1], **Kaan Boztug**[3], **Talal A. Chatila**[2], and **Isil B. Barlan**[1]

[1]Marmara University, Division of Pediatric Allergy/Immunology, Istanbul, Turkey

[2]Division of Immunology, Boston Children's Hospital and Department of Pediatrics, Harvard Medical School, Boston, MA, USA

[3]CeMM Research Center for Molecular Medicine of the Austrian Academy of Sciences, Vienna, Austria Department of Pediatrics and Adolescent Medicine, Medical University of Vienna, Vienna, Austria

Abstract

Purpose—Loss and gain of function (GOF) mutations in human signal transducer and activator of transcription 1 (STAT1) lead to distinct phenotypes. Although recurrent infections are common to both types of *STAT1* mutations, GOF mutations are distinguished by chronic mucocutaneous candidiasis and autoimmunity. However, the clinical spectra of *STAT1* GOF mutations continue to expand. We here describe two patients with *STAT1* GOF mutations presenting early in life with combined immunodeficiency (CID).

Methods—Clinical data and laboratory findings including immunophenotyping, level of interferon (IFN)-γ/IL-17$^+$ T cells, interferon-induced STAT1 phosphorylation and JAK inhibitor assays were evaluated. Sequencing of *STAT1* gene was performed by Sanger sequencer.

Results—Patient 1 (P1) had persistent oral candidiasis and cytomegalovirus (CMV) infection since 2 months of age, and later developed cavitary lung lesions due to *Mycobacterium tuberculosis*. Patient 2 (P2) presented with oral candidiasis and recurrent pneumonia at 4 months of age, and subsequently developed CMV pneumonitis. Both patients suffered heterozygous missense mutations in *STAT1*, leading to deleterious amino acid substitutions in the DNA binding domain (P1: c.1154C>T; p.T385M; P2. c.971G>T; p.C324F). Circulating CD4$^+$ T cells of both patients exhibited increased interferon-γ and decreased IL-17 expression as compared to controls. They also exhibited increased IFN-β and -γ-induced STAT1 phosphorylation that was reversed upon treatment with the JAK kinase inhibitor Ruxolitinib.

Corresponding author: Safa Baris, MD, Marmara University, Division of Pediatric Allergy/Immunology, Fevzi Çakmak Mah. No: 41, Pendik / Istanbul/Turkey. Phone: +90 216 625 78 11; Fax: +90 216 432 06 95.

*The authors contributed equally to the study.

Authors declare no conflict of interest.

Conclusion—*STAT1* GOF mutations may present early in life with CID, consistent with the clinical heterogeneity of the disease. JAK kinase inhibitors may potentially be useful in some patients as adjunct therapy pending definitive treatment with bone marrow transplantation.

Keywords

STAT1; gain-of function mutation; mucocutaneous candidiasis; combined immunodeficiency; autoimmunity; Ruxolitinib

Introduction

Signal transducer and activator of transcription 1 (STAT1) mediates the actions of many cytokines involved in mounting innate and adaptive immune responses to viruses and intracellular bacteria (1). *STAT1* is the target of heritable loss-of-function (LOF) or gain-of-function (GOF) mutations that give rise to distinct clinical phenotypes. While autosomal dominant *STAT1* LOF mutated patients suffer from infections with mycobacteria and other macrophage-bound bacteria but do not evidence undue susceptibility to viral infections, autosomal recessive hypomorphic *STAT1* LOF mutated patients are prone to both mycobacterial and viral infections. These mutations reflect failure of interferon (IFN)-γ- and IFN-α/β-mediated immunity, respectively (2-4). In contrast, autosomal dominant GOF mutations are prominently associated with chronic mucocutaneous candidiasis (CMC) and autoimmune phenomena, related to augmented T helper cell type 1 (T_H1) response and T helper cell type 17 (T_H17) deficiency (5-8).

CMC is a heterogeneous disorder with recurrent chronic *Candida* infections primarily involving nails, skin and oropharynx. CMC can be associated with several conditions including autoimmune polyglandular syndrome type 1, combined immunodeficiencies (CIDs), *DOCK8, IL12RB1, IL12B, CARD9, IL17F, IL17RA, IL17RC, ACT1, TYK2* and *STAT3* gene defects (8). The genetic repertoire of CMC has been further expanded by the identification of GOF mutations in *STAT1* gene which leads to defective T_H17 cell production and subsequent development of CMC (5, 6).

We report here 2 unrelated Turkish patients with autosomal dominant GOF mutations in *STAT1* gene; presenting with oral candidiasis complicated with recurrent CMV infections and cavitary mycobacterial lung infections resembling CID.

Methods

STAT1 mutation identification and sequencing

Whole exome sequencing was performed as described (9). *STAT1* sequences were derived from genomic DNA by polymerase chain reaction (PCR) amplification and sequenced bidirectionally using dye-terminator chemistry.

Antibodies and flow cytometry

Monoclonal antibodies (mAbs) to the following human proteins were used for staining: CD3 (UCHT1), CD4 (RPA-T4), IFN-γ (4S.B3), IL-17 (BL168) (Biolegend), phospho (p)-STAT1

(KIKSI0803), (all from eBioscience), STAT1 (246523; R&D Systems). Appropriate isotype controls were used in parallel. PBMCs were incubated with mAbs against surface markers for 30 min on ice. Intracellular staining with STAT1 mAb was performed using an eBioscience fixation/permeabilization kit according to the manufacturer's instructions. For p-STAT1 staining, PBMCs were stimulated for 20 min with appropriate cytokines in complete medium, fixed with 2% paraformaldehyde for 20 min on ice, permeabilized with 90% methanol for 30 min on ice and stained using CD3, CD4 and p-STAT1 mAbs in PBS for 30 min. For cytokine detection, cell suspensions were incubated with Phorbol myristate acetate (PMA) (Sigma-Aldrich; 50 ng/mL), Ionomycin (Sigma-Aldrich; 500 ng/mL) and GolgiPlug™ (BD Biosciences; according to manufacturer's instructions) for 4 h in complete medium before surface staining. Permeabilization and intracellular IFN-γ and IL-17 staining was carried out using an eBioscience Fixation/Permeabilization kit as described above. Data were collected with an LSRFortessa™ cytometer (BD Biosciences) and analyzed with FlowJo software (Tree Star, Inc.).

JAK kinase inhibitor treatment

PBMCs were incubated for 4h in the presence of different concentrations of Ruxolitinib, a JAK1/2 inhibitor (Selleckchem; 10 nM, 100 nM), or vehicle (Dimethyl Sulfoxide) alone prior to stimulation with recombinant human IFN-β (Miltenyi; 20 ng/ml).

Cell proliferation assay

EdU (5-ethynyl-2'-deoxyuridine) was added at 10mM to PBMCs (1×10^6 cells) and the cells were cultured in 96-well plates for 72 hours. Cell proliferation was assessed by flow cytometry using Click-iT EdU imaging kit (Invitrogen, Paisley, UK) according to the manufacturer's instructions.

Statistical Analysis

Comparisons between the patient and healthy controls were analyzed using the unpaired Student's t-test and two-way ANOVA with post-test analysis. Two-sided p-values less than 0.05 were considered statistically significant.

Results

Case reports

Patient 1 (P1)—A 2-year-old girl was referred to clinic at 2 months of age due to recurrent urosepsis and refractory candidiasis since one week of age despite antifungal therapy. Physical examination was notable for hepatosplenomegaly, oral thrush and hypopigmented skin lesions. Chest X-ray showed bilateral interstitial infiltration. Concomitantly, cytomegalovirus (CMV) PCR was detected in blood with 23,457 copy/ml. Despite favorable clinical response to a total of 3 weeks intravenous gancyclovir therapy, pneumonia and CMV positivity relapsed and complicated with acute respiratory distress syndrome. Although, patient's phenotype was resembled CID, she had normal blood count with differentials and serum immunoglobulin levels. Evaluation of lymphocyte subsets was normal except for reversed CD4/CD8 ratio, low naïve $CD3^+$, $CD8^+$, and memory switched $CD19^+$ cells (Table 1). Proliferative response of lymphocytes to CD-mix and phytohemagglutinin (PHA) was

found to be comparable with age matched healthy subject. During the follow-up cavitary lung lesions accompanied by consolidation were demonstrated by imaging of the lung (Fig. 1). *Mycobacterium tuberculosis* complex was identified in bronchoalveolar lavage fluid by PCR. Family history was notable for latent tuberculosis (TB) infection in her mother. In addition, her BCG vaccination (*Mycobacterium Bovis*) had been postponed due to a suspicion of CID. Presence of persistent oral candidiasis, Mycobacterial lung disease and CMV infection led us to investigate Mendelian susceptibility to mycobacterial diseases-related genes. Whole exome sequencing analysis revealed a *de novo* heterozygous variant, confirmed by Sanger sequencing, in the DNA binding domain (DBD) of *STAT1*; c.1154C>T causing a T385M amino acid substitution in STAT1, previously reported as a pathogenic GOF mutation (Fig. 1A) (10-12).

To control the mycobacterial infection, anti-TB therapy was started. However, it was interrupted several times due to elevated liver enzymes. Her liver biopsy found to be compatible with hepatitis in the absence of CMV inclusion bodies and acid resistant bacilli. Autoantibodies including anti-liver-kidney microsome (LKM), anti-smooth muscle (ASM), anti-soluble liver antigen (SLA) and anti-parietal antibodies were all found to be negative. Persistently elevated liver enzymes along with anti-nuclear antibody (ANA) positivity (1/100) led us to initiate corticosteroid therapy (2mg/kg/day) which resulted in a favorable response with a significant decrease in liver function tests. Considering the severe clinical course, currently, the patient is being evaluated for hematopoietic stem cell transplantation (HSCT) from full-matched healthy sibling.

Patient 2 (P2)—A 3-year-old male was born at 36 weeks of pregnancy after in vitro fertilization required admission in neonatal intensive care unit for 18 days due to respiratory insufficiency. Recurrent pneumonia and persistent oral candidiasis were prominent since 4 month of age. At 7 months, he was admitted due to prolonged fever, dyspnea and hepatomegaly. At that time, CMV infection was diagnosed by PCR (9500 copy/ml), which responded well to intravenous gancyclovir therapy. Oral candidiasis responded to oral fluconazole therapy.

At 9 months of age, low serum IgM (13 mg/dl), low IgA (<5 mg/dl) and normal IgG (504 mg/dl) were observed and lymphocyte immunophenotyping revealed a decreased CD4/CD8 T cell ratio but normal T, B and NK cells. Naive CD4, CD8 T cells and PHA stimulated T cells proliferation were found to be lower than healthy control (Table 1). Until now he had several hospital admissions due to lower respiratory tract infections along with blood CMV PCR positivity despite valganciclovir prophylaxis. No other fungal or bacterial microorganisms were detected to be responsible for the lung involvement. The lung chest computed tomography showed bilaterally upper and middle lobe infiltration, interstitial involvement and glossy patch appearances which were compatible with CMV infection (Fig. 1B). Abdominal ultrasound revealed splenomegaly, liver parenchymal heterogeneity and multiple nodular calcifications. The patient received intravenous immunoglobulin therapy, board spectrum antibiotics and gancyclovir to control several episodes of respiratory tract infections. Whole exome sequencing analysis revealed heterozygous *de novo STAT1* missense mutation (c.971G>T; p.C324F) at DBD which was later confirmed by Sanger sequencing (Fig. 1A). This mutation, which was not found in dbSNP 138 or the 1000

Genomes Project, led to the substitution of a highly conserved cysteine amino acid at position 324 of STAT1 with phenylalanine. The mutation was predicted to have damaging impact on protein function by PolyPhen-2 with a score of 0.977 (sensitivity: 0.76; specificity: 0.96). Due to poor disease control and quality of life, the patient was transplanted from full matched unrelated donor and still well at 3 months after HSCT.

STAT1 phosphorylation—To investigate the functional consequences of patient STAT1 mutations, we first demonstrated the normal expression of total STAT1 protein in $CD4^+$ T cells of patients and healthy control (Fig. 2A). Subsequently, we analyzed STAT1 phosphorylation in patient and control T cells at baseline and following stimulation with IFN-β. At baseline, STAT1 was minimally phosphorylated to a similar extent in patient and control T cells (Fig. 2B). However, IFN-β treatment resulted in STAT1 hyperphosphorylation in patient as compared to control T cells (Fig. 2C). Washing away of IFN-β following cell treatment revealed that whereas at 1 hour post cytokine wash the pSTAT1 signal declined by about 70% in the T cells of the two patients, it remained increased as compared to that of control T cells in which the pSTAT1 signal declined even more precipitously (up to 85%). However, the pSTAT1 signals of patients and control T cells merged thereafter, indicating equivalent decay (Fig. 2D, E). Overall, these results suggest that the increased cytokine-induced STAT1phospohrylation in patient T cells is contributed to by both increased JAK kinase-mediated phosphorylation activity and delayed dephosphorylation of the mutant STAT1 proteins.

T_H cell cytokine expression—We analyzed the impact of patient *STAT1* GOF mutations on IFN-γ and IL-17 cytokine expression by $CD4^+$ peripheral blood T cells. Both patients manifested significantly increased frequencies of circulating IFN-γ^+CD4^+ T cells, and decreased frequencies of IL-17^+CD4^+ T cells as compared to age matched healthy controls (Fig. 3A, B). These results are consistent with previously reported changes in both subsets in patients with *STAT1* GOF mutations, related to potentiation of T_H1 and antagonism of T_H17 cell skewing.

The Janus kinase 1/2 inhibitor Ruxolitinib suppresses dysregulated $STAT1^{T385M}$ phosphorylation induced by IFN-β—The JAK inhibitor Ruxolitinib, which primarily targets JAK1/2, has been used to control dysregulated JAK/STAT activity (13, 14). We therefore examined the capacity of Ruxolitinib to suppress augmented $STAT1^{T385M}$ phosphorylation in $CD4^+$ T cells response to IFN-β stimulation. Ruxolitinib suppressed augmented IFN-β-induced $STAT1^{T385M}$ phosphorylation in patient P1 $CD4^+$ T cells within a concentration dependent manner, while having modest effects on STAT1 phosphorylation in control $CD4^+$ T cells (Fig. 4 A, B). These results are consistent with the GOF property of $STAT1^{T385M}$ and indicated that inhibition of JAK kinase activation may serve as a potential therapeutic modality for these patients.

Discussion

In this report, we described two patients with heterozygous GOF mutations in *STAT1* gene; both patients have severe CMV infections, oral candidiasis without obvious autoimmunity. Severe lung involvement was observed due to Mycobacterial infection in P1 and CMV

infection in both patients. Cases presented here led us to suggest that *STAT1* gene defects have broader clinical spectrum than initially considered which can be overlapped with CID phenotype.

Previously, AD *STAT1* mutations had been linked to genetic susceptibility to mycobacterial disease (4). However, it has been shown that AD *STAT1* GOF mutations in coiled-coil and DBD of *STAT1* were clinically associated with CMC (5-8, 10, 15). Recently, a case with CMC was reported with a SH2 domain mutation causing GOF in STAT1 protein (16). In this report we describe two patients with GOF mutations presenting early in life with a CID picture. One mutation, T385M, has already been reported by several groups as GOF (10-12). While one report suggested T385M is a LOF mutation, our own results are consistent with a GOF phenotype of this mutation, as revealed by its association with cytokine-induced STAT1 hyperphosphorylation, exaggerate T_H1 and decreased T_H17 responses (17). The second mutation, C324F, is a newly identified mutation that also resulted in increased cytokine-induced STAT1 phosphorylation and impaired IL-17 production, consistent with its GOF property. Recently, an international STAT1 GOF study group published clinical, genetic and laboratory findings of 274 patients with AD *STAT1* GOF mutations (18). In this cohort, C324R mutation has been reported as GOF. This reported mutation and our C324F alleles demonstrate the importance of this highly conserved residue for STAT1 protein's function.

Our two patients presented at early life period with oral candidiasis complicated with severe CMV infection that resulted in chronic lung disease. The clinical picture of our patients was consistent with a CID phenotype. Increased susceptibility to herpes simplex, varicella zoster virus, respiratory syncytial virus, CMV and Epstein Barr virus (EBV) has been reported in association with *STAT1* GOF mutations(12, 15, 19). Toubiana et al. reported CMV or EBV infections in 15% of the patients (18). Previously, T385M mutation was reported to present with fungal infections or respiratory manifestations, but also with progressing to combined immunodeficiency (10-12). Our patients extend the spectrum of the disease. The high rate of candidial infection probably was explained with impaired IL-17 protective immune response (6). Furthermore, in this kind of mutation, severe dimorphic yeast infections (coccidioidomycosis and histoplasmosis) can be caused by abnormal regulation of IFN-γ responses (10). On the other hand, the variety of infections might be associated with progressive lymphopenia, abnormal T cell functions, loss of memory B cells, and hypogammaglobulinemia as in our patients (15).

Mycobacterial infections have been previously associated with AD or AR *STAT1* LOF mutations (4). Interestingly, patient P1, who has a $STAT1^{T385M}$ mutation, developed cavitary tuberculosis at 9 months of age. Although it has been previously shown that GOF mutations enhance IFN-γ inducible target gene expression, restimulation with IFN-γ maybe give rise to impaired IFN-γ responses. This mechanism can partially explain the susceptibility to mycobacterial infections (10).

In our patients disease symptoms presented early in life. Despite anti-bacterial, viral and fungal therapies, the patients continued to be in poor health with frequent hospital admissions, leading to consideration of HSCT. There are six patients with *STAT1* GOF

mutation who underwent HSCT due to poor disease control (18, 20). However, four of them died after several months due to disseminated CMV infection, hemaphagocytic lymphohistiocytosis and pulmonary complications. Although Patient P2 is doing well after 3 months of transplantation, further follow-up period needed to make a conclusion for this kind of therapy in patients with *STAT1* GOF.

Other therapeutic modalities have been reported for STAT1 GOF patients. Oral Ruxolitinib, a JAK1/2 kinase family protein tyrosine kinase inhibitor was used in a patient with a *STAT1* GOF mutation, CMC and alopecia areata, in whom a complete clinical remission was achieved after 12 weeks of treatment (13). However, the CMC returned within 2 weeks after discontinuation of treatment, despite oral fluconazole. We showed that in-vitro treatment with Ruxolitinib significantly decreased the exaggerated cytokine-induced p-STAT1 response in $CD4^+$ T cells of patient P1, suggesting that this therapeutic modality may be useful in case HSCT is unavailable. In addition, case reports with *STAT1* GOF mutations have shown that treatment with either granulocyte-colony stimulating factor or granulocyte monocyte-colony stimulating factor may improve the generation of T_H17 cells and recovery from fungal infections (11).

In conclusion, the clinical presentations of our patients with severe, early onset CID support the notion that *STAT1* GOF mutations give rise to a wide range of disease phenotypes including fungal, mycobacterial infections and autoimmunity as well as combined immunodeficiency.

Acknowledgments

This manuscript is dedicated to the memory of Professor Dr. Işıl Berat Barlan (1958-2015).

This work was supported by the National Institutes of Health (R01 AI085090), to T.A.C.

References

1. Casanova JL, Holland SM, Notarangelo LD. Inborn errors of human JAKs and STATs. Immunity. 2012 Apr 20; 36(4):515–28. [PubMed: 22520845]
2. Dupuis S, Dargemont C, Fieschi C, Thomassin N, Rosenzweig S, Harris J, et al. Impairment of mycobacterial but not viral immunity by a germline human STAT1 mutation. Science. 2001 Jul 13; 293(5528):300–3. [PubMed: 11452125]
3. Dupuis S, Jouanguy E, Al-Hajjar S, Fieschi C, Al-Mohsen IZ, Al-Jumaah S, et al. Impaired response to interferon-alpha/beta and lethal viral disease in human STAT1 deficiency. Nat Genet. 2003 Mar; 33(3):388–91. [PubMed: 12590259]
4. Boisson-Dupuis S, Kong XF, Okada S, Cypowyj S, Puel A, Abel L, et al. Inborn errors of human STAT1: allelic heterogeneity governs the diversity of immunological and infectious phenotypes. Curr Opin Immunol. 2012 Aug; 24(4):364–78. [PubMed: 22651901]
5. van de Veerdonk FL, Plantinga TS, Hoischen A, Smeekens SP, Joosten LA, Gilissen C, et al. STAT1 mutations in autosomal dominant chronic mucocutaneous candidiasis. N Engl J Med. 2011 Jul 7; 365(1):54–61. [PubMed: 21714643]
6. Liu L, Okada S, Kong XF, Kreins AY, Cypowyj S, Abhyankar A, et al. Gain-of-function human STAT1 mutations impair IL-17 immunity and underlie chronic mucocutaneous candidiasis. J Exp Med. 2011 Aug 1; 208(8):1635–48. [PubMed: 21727188]
7. Hori T, Ohnishi H, Teramoto T, Tsubouchi K, Naiki T, Hirose Y, et al. Autosomal-dominant chronic mucocutaneous candidiasis with STAT1-mutation can be complicated with chronic active hepatitis and hypothyroidism. J Clin Immunol. 2012 Dec; 32(6):1213–20. [PubMed: 22847544]

8. Marodi L, Cypowyj S, Toth B, Chernyshova L, Puel A, Casanova JL. Molecular mechanisms of mucocutaneous immunity against Candida and Staphylococcus species. J Allergy Clin Immunol. 2012 Nov; 130(5):1019–27. [PubMed: 23040277]

9. Salzer E, Santos-Valente E, Klaver S, Ban SA, Emminger W, Prengemann NK, et al. B-cell deficiency and severe autoimmunity caused by deficiency of protein kinase C delta. Blood. 2013 Apr 18; 121(16):3112–6. [PubMed: 23319571]

10. Sampaio EP, Hsu AP, Pechacek J, Bax HI, Dias DL, Paulson ML, et al. Signal transducer and activator of transcription 1 (STAT1) gain-of-function mutations and disseminated coccidioidomycosis and histoplasmosis. J Allergy Clin Immunol. 2013 Jun; 131(6):1624–34. [PubMed: 23541320]

11. Dotta L, Scomodon O, Padoan R, Timpano S, Plebani A, Soresina A, et al. Clinical and immunological data of nine patients with chronic mucocutaneous candidiasis disease. Data in brief. 2016 Jun.7:311–5. [PubMed: 26981552]

12. Soltesz B, Toth B, Shabashova N, Bondarenko A, Okada S, Cypowyj S, et al. New and recurrent gain-of-function STAT1 mutations in patients with chronic mucocutaneous candidiasis from Eastern and Central Europe. J Med Genet. 2013 Sep; 50(9):567–78. [PubMed: 23709754]

13. Higgins E, Al Shehri T, McAleer MA, Conlon N, Feighery C, Lilic D, et al. Use of ruxolitinib to successfully treat chronic mucocutaneous candidiasis caused by gain-of-function signal transducer and activator of transcription 1 (STAT1) mutation. J Allergy Clin Immunol. 2015 Feb; 135(2):551–3. [PubMed: 25662309]

14. Liu Y, Jesus AA, Marrero B, Yang D, Ramsey SE, Montealegre Sanchez GA, et al. Activated STING in a vascular and pulmonary syndrome. The New England journal of medicine. 2014 Aug 7; 371(6):507–18. [PubMed: 25029335]

15. Uzel G, Sampaio EP, Lawrence MG, Hsu AP, Hackett M, Dorsey MJ, et al. Dominant gain-of-function STAT1 mutations in FOXP3 wild-type immune dysregulation-polyendocrinopathy-enteropathy-X-linked-like syndrome. J Allergy Clin Immunol. 2013 Jun; 131(6):1611–23. [PubMed: 23534974]

16. Sobh A, Chou J, Schneider L, Geha RS, Massaad MJ. Chronic mucocutaneous candidiasis associated with an SH2 domain gain-of-function mutation that enhances STAT1 phosphorylation. J Allergy Clin Immunol. 2016 Feb 29.

17. Sharfe N, Nahum A, Newell A, Dadi H, Ngan B, Pereira SL, et al. Fatal combined immunodeficiency associated with heterozygous mutation in STAT1. J Allergy Clin Immunol. 2014 Mar; 133(3):807–17. [PubMed: 24239102]

18. Toubiana J, Okada S, Hiller J, Oleastro M, Lagos Gomez M, Aldave Becerra JC, et al. Heterozygous STAT1 gain-of-function mutations underlie an unexpectedly broad clinical 336 phenotype: an international survey of 274 patients from 167 kindreds. Blood. 2016 Apr 25.

19. Mizoguchi Y, Tsumura M, Okada S, Hirata O, Minegishi S, Imai K, et al. Simple diagnosis of STAT1 gain-of-function alleles in patients with chronic mucocutaneous candidiasis. J Leukoc Biol. 2014 Apr; 95(4):667–76. [PubMed: 24343863]

20. Aldave JC, Cachay E, Nunez L, Chunga A, Murillo S, Cypowyj S, et al. A 1-year-old girl with a gain-of-function STAT1 mutation treated with hematopoietic stem cell transplantation. J Clin Immunol. 2013 Nov; 33(8):1273–5. [PubMed: 24105462]

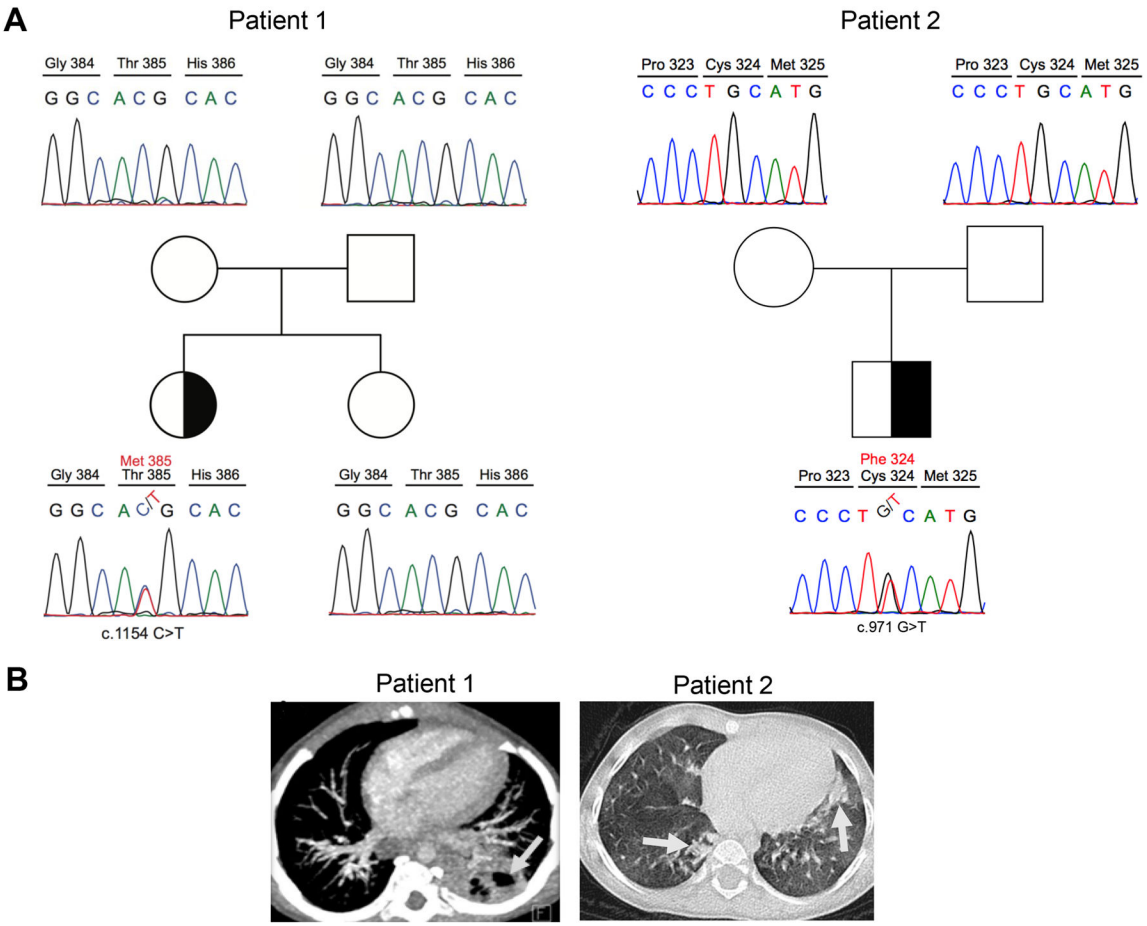

Figure 1. Identification of de novo autosomal dominant *STAT1* mutations in two patients with early onset CID

(**A**) Patient 1 (right site) and patient 2 (left site) families. The half-filled symbol indicates the heterozygous carrier; open symbols refer to wild type individuals. Males and females are distinguished by squares and circles, respectively. (**B**) Chest computed tomography of STAT1 GOF patients. Cavitary lung lesion (3.5 cm) in left lower lobe of patient 1 (Gray arrow). Bilaterally lobe infiltration, interstitial involvement and glossy patch appearances of patient 2 (Gray arrows).

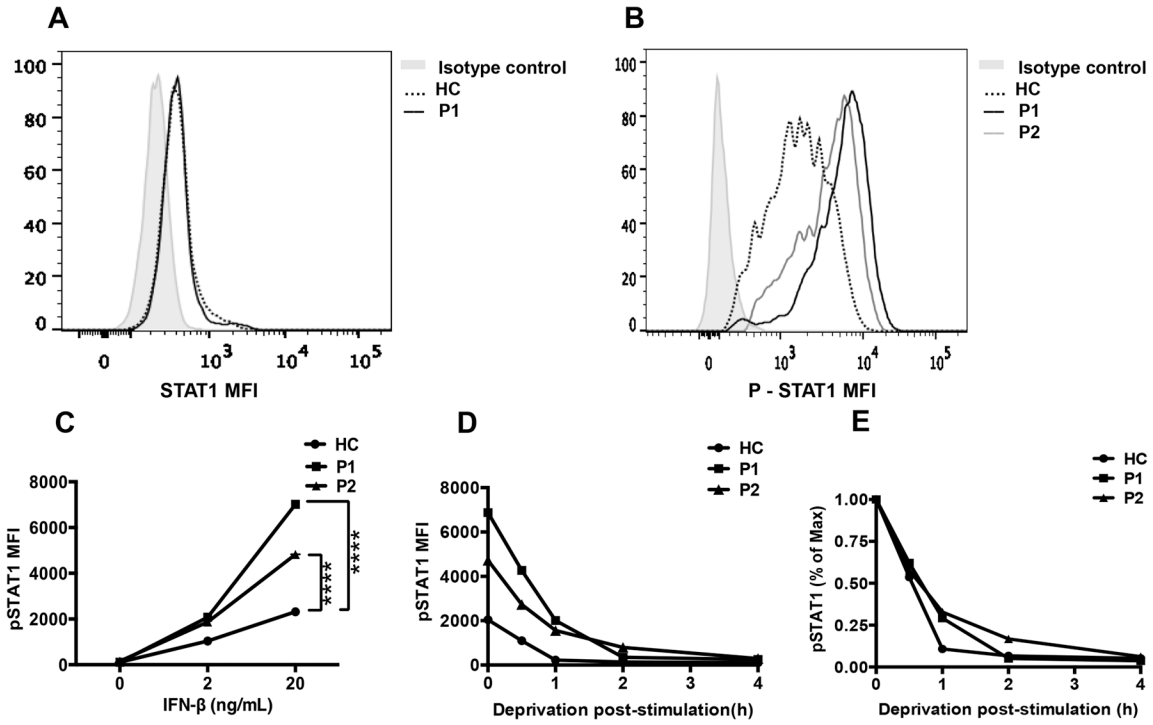

Figure 2. Gain of function mutations in *STAT1* (T385M, C324F) lead to STAT1 hyperphosphorylation

(A) Total p-STAT1 expression in $CD4^+$ T cells stimulated with IFN-β (20 ng/mL) by flow cytometry in patients (P1, P2) and healthy control. (B) STAT1 expression in $CD4^+$ T cells in patient P1 and control. (C) The dose response curve of STAT1 phosphorylation induced with IFN-β in patients and control $CD4^+$ T cells. (D) Dephosphorylation kinetics of p-STAT1 in response to deprivation of IFN-β in $CD4^+$ T cells represented as absolute MFI (D) and normalized to maximum expression prior to deprivation (E). **** $p<0.0001$ by two way ANOVA.

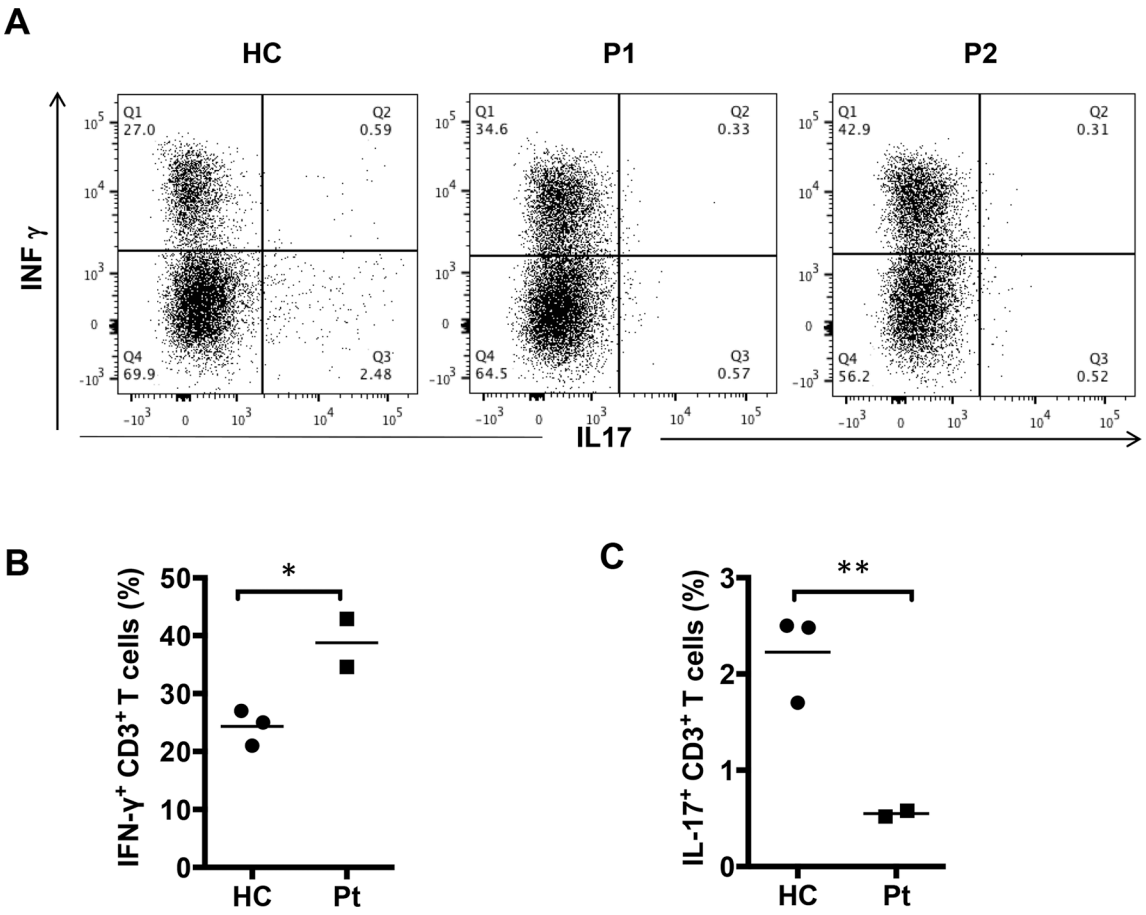

Figure 3. Exacerbated T_H1 and impaired T_H17 responses in *STAT1* GOF mutations

(A) Flow cytometric analyses of IL-17 and IFN-γ secretion by peripheral $CD4^+$ cells from controls and our patients. (B) The frequencies of IFN-γ and IL-17 producing $CD4^+$ cells in three healthy controls and two patients. * $p<0.05$ and ** $p<0.01$ by unpaired two-tailed Student's *t*-test.

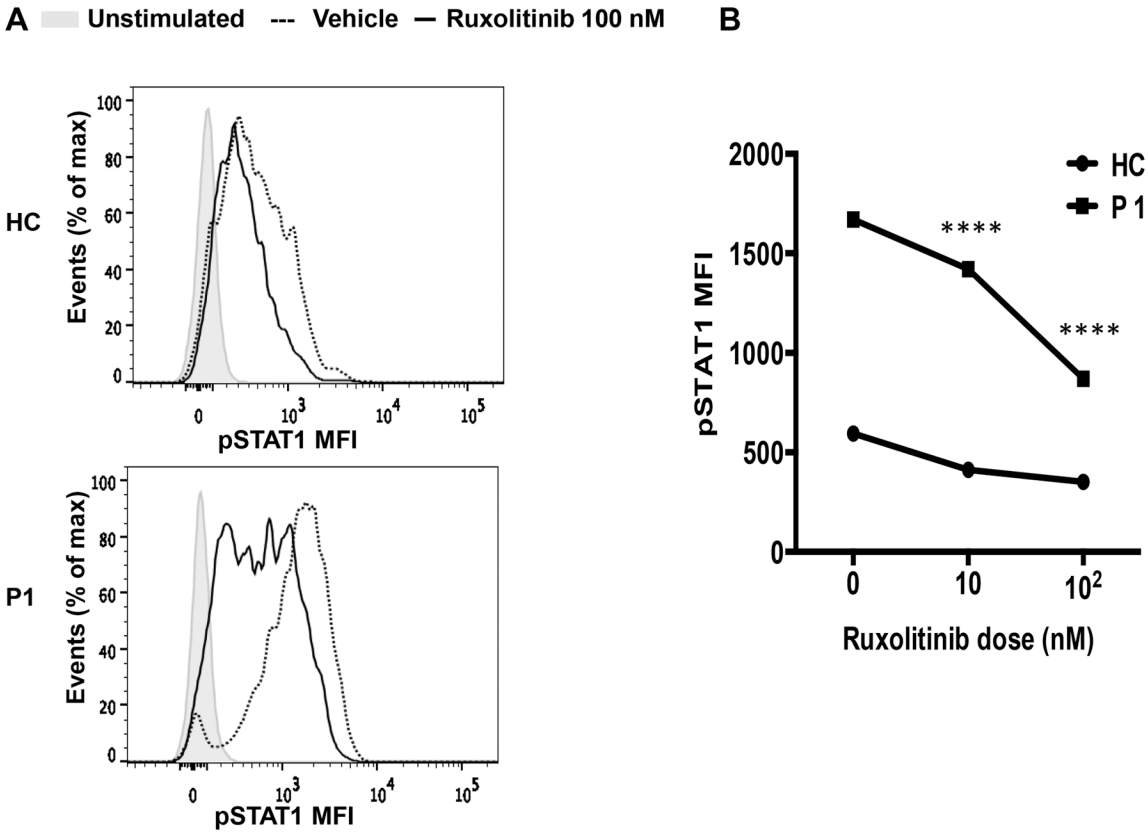

Figure 4. *In vitro* inhibition of STAT1 phosphorylation by Janus kinase inhibitor Ruxolitinib

(A) Expression of p-STAT1 in $CD4^+$ T cells from healthy control and patient pretreated for 4 hours with 100 nM concentration of Ruxolitinib (black line) or vehicle (DMSO) then stimulated with IFN-β (20 ng/mL). The plain grays correspond to unstimulated cells. p-STAT1 mean fluorescence intensity (MFI) expressed in $CD4^+$ T cells of healthy control and patient P1 as percent of maximum vehicle, Ruxolitinib 10 nM or 100 nM concentrations shown in (B). **** $p<0.0001$ two way ANOVA with posttest analysis.

Table 1
The clinical and Immunological features of the patients

Patients (Age)	P1 (12 months)	P2 (12 months)	Reference values
Sex	Male	Male	-
Age at onset	2 months	4 months	-
Chronic mucocutaneous candidiasis	Oral	Oral	-
Other Infections	- Cytomegalovirus - Mycobacterium tuberculosis - Pneumonia - Urosepsis	- Cytomegalovirus - Pneumonia	-
Autoimmunity	- Hepatitis	-	-
Others	- Cavitary lung lesion - Hepatosplenomegaly - Hypopigmented skin lesions	- Interstitial lung disease - Hepatosplenomegaly - Liver nodular calcifications	-
Lymphocyte numbers (cells/μl)	5900	3300	2600-10400
Immunoglobulins (mg/dL)			
IgG	616	949	304-1231
IgM	55	137	32-203
IgA	20	43	7-123
IgE (IU/L)	9.8	8	2-97
Immunophenotyping			
$CD3^+$ cells (%, cells/μl)	75 (4425)	79 (2607)	54-76 (1600-6700)
$CD3^+CD4^+$ (%, cells/μl)	30 (1770)	35 (1155)	31-54 (1000-4600)
$CD3^+CD8^+$ (%, cells/μl)	33 (1947)	43(1419)	12-28(400-2100)
$CD4^+/CD8^+$ ratio	0.9	0.8	1.3-3.9
$CD3^+CD4^+CD45RA^+$ (%)	33	15	77-94
$CD3^+CD4^+CD45RO^+$ (%)	40	38	3-16
$CD3^+CD8^+CD45RA^+$ (%)	40	32	75-97
$CD3^+CD8^+CD45RO^+$ (%)	67	41	02-12
$CD19^+$ cells (%, cells/μl)	18.6 (1097)	13 (429)	14-39 (700-2500)
Naïve $CD19^+CD27^-IgD^+$ (%)	95	89	76-94
UCSM $CD19^+CD27^+IgD^+$ (%)	3.8	5.1	3-10.7
CSM $CD19^+CD27^-IgD^-$ (%)	0.4	2	1.4-11.9
$CD16^+/CD56^+$ cells % (n)	4.3	4.2	2-14
Proliferation (%)(PHA)	73	2	58
Autoantibodies	ANA (1/100)	-	N<1/100
Mutation (Domain)	T385M (DBD)	C324F (DBD)	-

Abbreviations: PHA: phytohemagglutinin, UCSM: Unclass-switched memory, CSM: Class-switched memory, ANA: Anti-nuclear antibody, DBD: DNA binding domain.